Available online at www.sciencedirect.com
ScienceDirect
Polymer 49 (2008) 1823–1830
polymer
www.elsevier.com/locate/polymer

Multicomponent vapor deposition polymerization of poly(methyl methacrylate) in an axisymmetric vacuum reactor

Xichong Chen, Mitchell Anthamatten*

Department of Chemical Engineering, University of Rochester, 206 Gavett Hall, Rochester, NY 14627, United States

Received 12 September 2007; received in revised form 7 February 2008; accepted 16 February 2008
Available online 21 February 2008

Abstract

An axisymmetric, multicomponent initiated chemical vapor deposition (i-CVD) apparatus was designed to study the vapor-phase growth of glassy poly(methyl methacrylate) (PMMA) films. Preheated monomer (methyl methacrylate) and initiator (*t*-butyl peroxide) vapors were metered into a pressure-controlled reaction chamber. Inside the chamber, gases pass through a high-temperature hot-zone where primary free radicals are formed. The gas mixture then condenses and polymerizes on a back-cooled target substrate. Key reactor operating parameters were systematically varied to understand film growth kinetics. These include the hot-zone temperature, reactor base-pressure, substrate temperature, and the monomer/initiator molar feed ratio. Polymer deposition requires good thermal contact between feed gases and the hot-zone. Packed with glass beads, the hot-zone reactor resulted in more efficient initiation and film growth. Experiments also show that polymer deposition rate is limited by thermal initiation of primary free radicals, transport of primary free radicals to the target substrate, and by monomer adsorption. Size exclusion chromatography of deposited polymers is used to relate molecular weight to the monomer-to-initiator feed ratio. The addition of a third vapor component, 1-butanol, was also found to affect polymer molecular weight.

Keywords: Free radical polymerization; Thin films; Vapor deposition

1. Introduction

Chemical vapor deposition (CVD) of polymers involves the condensation and reaction of reactive species onto a target substrate. Vapor processing is well suited to modify surface properties of bulk materials, for example scratch-resistant and antimicrobial coatings [1], or to prepare thin film devices such as thin film transistors [2,3], photovoltaic cells [4], and gas separation membranes [5]. Vapor-phase processing is differentiated from solution-based techniques in many ways: (1) film growth is generally slow (~μm/h), enabling films to be grown to precisely desired thicknesses; (2) film properties can be tuned by adjusting the molar flux ratios of gaseous precursor components; (3) polymers can be coated onto rough substrates or even onto complex 3D geometries; and (4) vapor-derived processes are "solventless" and are attractive from an environmental standpoint.

Vapor deposition of both condensation and addition polymers has been performed in the absence of a plasma and resulted in polymer chains that are chemically similar to their solution analogs. Condensation polymers including, polyamides [6], polyimides [7–9], and polybenzoxazoles [10], can be grown by vacuum codeposition of reactive monomers to yield glassy, nearly isotropic films [11] with less orientation than is typically observed in solution processed films [12]. The resulting macromolecules are lower in molecular weight than their solution analogs [13].

Initiated chemical vapor deposition (i-CVD) is a technique used to carry out addition polymerization [14–21]. A gas mixture of monomers and free radical initiators is fed at moderately low pressures (~1 Torr) over a resistively-heated filament, and initiator molecules are thermally activated by the filament. Both monomers and initiators diffuse to a target substrate, and there, they undergo free radical polymerization to

* Corresponding author. Tel.: +1 585 273 5526; fax: +1 585 273 1348.
E-mail address: anthamatten@che.rochester.edu (M. Anthamatten).

0032-3861/$ - see front matter © 2008 Elsevier Ltd. All rights reserved.
doi:10.1016/j.polymer.2008.02.027

form linear chains. Depending on the initiator-to-monomer molar flux ratio and the chamber's operating pressure, coating rates are typically high (~5 μm/h) and high molecular weight ranges are obtained compared to other vapor deposition techniques. To date, this technique has been demonstrated for a wide range of polymers including, for example, poly(alkyl acrylates) [14,16–18], poly(glycidyl methacrylate) (PGMA) [21], poly(oxymethylene) [20], and fluorocarbon films that are spectroscopically similar to PTFE [19].

Prior studies of i-CVD have involved horizontal flow of monomer and initiator gases across a heated-filament array which is positioned horizontally above a cooled target substrate. Thermal decomposition of initiator molecules into free radicals occurs near the hot-filament array. Generated free radicals and unreacted monomer molecules adsorb onto the cooled substrate and irreversibly undergo polymerization. Recent studies of hot-filament i-CVD indicate that polymerization is limited by monomer adsorption and, within the adsorbed layer, reaction kinetics are analogous to bulk-phase free radical polymerization [22].

In this study, we employ an alternate reactor configuration to perform initiated chemical vapor deposition process that avoids a hot-filament altogether. First, gas precursors are passed vertically through a tubular packed-bed hot-zone. The purpose of the hot-zone is to activate free radical initiator molecules. The hot-zone is isothermal, eliminating hot-spots that could result in thermal degradation of initiator or monomer species. Following the hot-zone, the gas mixture is perpendicularly directed at a cooled target substrate, and reactants condense and polymerize on the substrate, analogous to the hot-filament process. Unreacted gases follow axisymmetric streamlines around substrate and then exit the reactor to the vacuum pump. This flow configuration was chosen to minimize mass transfer resistance to the substrate, to further decouple initiation and polymerization, and to improve film uniformity. The aim of the present study is to understand how reactor operating parameters are related to film growth rates and polymerization characteristics. As a model system, glassy films of poly(methyl methacrylate) (PMMA) are grown using this new reactor configuration.

PMMA is a widely studied, optically clear, room temperature polymer glass with several thin film applications. It is usually synthesized by solution free radical polymerization of methyl methacrylate monomer, and its reaction kinetics are well known. Applications of PMMA include protective and transparent coatings, bonding adhesives, and low κ dielectric layers [23].

PMMA can be fabricated into glassy, porous membranes using thermal-induced phase separation (TIPS) techniques [24,25]. TIPS involves rapid quenching of a polymer solution to a temperature where spinodal decomposition occurs, resulting in a glassy, two-phase microstructure. Porous PMMA membranes can also be fabricated using non-solvent induced phase separation (NIPS) [26,27] where phase splitting is induced by raising the non-solvent concentration. Polymerization-induced phase separation (PIPS) is another common strategy to form two-phase, structured polymers that have been used to create interpenetrating networks [28] and toughened amorphous glasses [29]. A multicomponent i-CVD system could open the door to vapor processing of porous polymers and other structured polymer glasses.

A second objective of the current study is to demonstrate how this reactor design is suited to explore depositions involving multiple components. Multicomponent i-CVD is demonstrated by co-condensing 1-butanol during the growth of PMMA films. Since 1-butanol is non-reactive and has a relatively high vapor pressure, it can be easily removed following deposition. Here we discuss how that presence of 1-butanol affects the molecular weight of as-deposited films. This result is the first step toward developing i-CVD as a technique to survey porous and structured polymer thin films with tunable morphologies.

2. Experimental

2.1. Materials

Methyl methacrylate (MMA) monomer (Alpha Aesar, 99% purity), *t*-butyl peroxide (Sigma-Aldrich, 97% purity), and 1-butanol (J. T. Baker, 99.99% purity) were all used as received, without further purification. Silicon wafers (7.62 cm diameter) or glass slides were used as the substrates for deposition runs. Wafers (Silicon International) were used as received. Glass slides were cleaned by soaking in a base-bath and then were vacuum-dried for overnight before each deposition.

2.2. i-CVD axisymmetric reactor design

Fig. 1 is a drawing of the axisymmetric i-CVD reactor used in this study. The reactor consists of a 27.90 cm diameter aluminum base-plate that supports a glass cylinder, 27.90 cm in length, with an aluminum top. Vacuum is achieved using a mechanical pump (BOC Edwards) through a pump-out port on the reactor, positioned opposite to the feed port. Reactor pressure is controlled using a downstream throttle valve (MKS Instruments) together with a Baratron capacitance manometer (MKS Instruments). Up to four different reagent gases can be supplied from separate bottles on a manifold on the up-stream side of the reactor. Reagent gases can be individually heated to ensure that supply-side vapor pressures are high enough to sustain steady flow. Reagent flowrates are regulated, prior to mixing, using separate mass-flow controllers. After mixing the reagents outside of the reactor, they are fed into the reactor through a heated transfer line (Heaters Controller and Sensors, Ontario, Canada). Upon entering the reactor, reagent gases are fed into a hot-zone consisting of an aluminum cylinder tube (ID = 11.43 cm). A band heater, combined with a temperature controller and read-out (Omega CN9000A), was used to regulate the hot-zone temperature. The distance between substrate and hot-zone was kept at 7.62 cm. The hot-zone can be packed with packing material to improve heat transfer to the supply gases. A porous aluminum gas diffuser, placed at the end of the hot-zone, is used to improve the outlet gas-flow uniformity. The distance between the hot-zone and the substrate is adjustable. The substrate can be glass slides or wafers up to 18 cm in

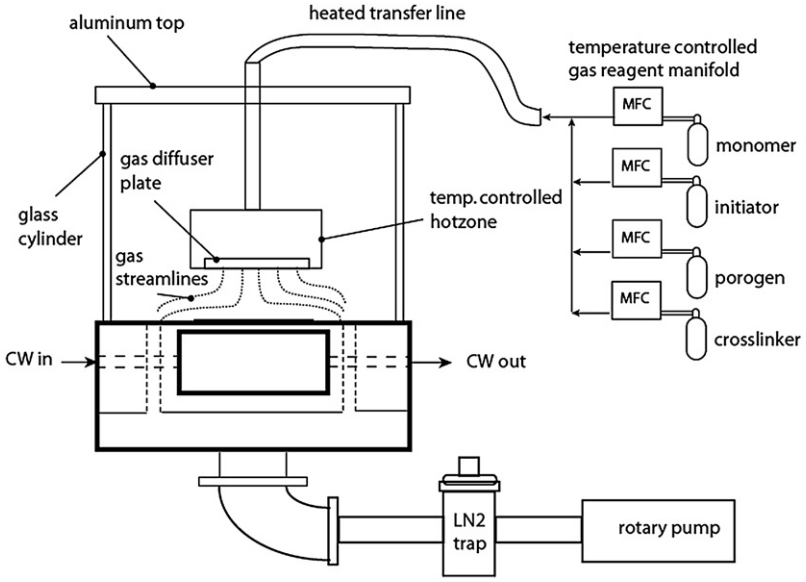

Fig. 1. Schematic of custom-built, axisymmetric i-CVD apparatus. Gas reagents are fed into a temperature-controlled hot-zone and are directed perpendicularly toward a cooled substrate.

diameter. The substrate temperature is controlled by backside cooling using a recirculating chiller/heater unit (Neslab RTE 740). The substrate temperature is also influenced by radiant heat transfer from the hot-zone and, to a lesser extent, by heat transfer from reagent gases. During operation, the substrate temperature, measured using a hand-held IR thermometer, was found to be about 5 °C warmer than the chiller temperature.

2.3. Deposition of PMMA films

During a typical experiment, the system was first pumped down to the operating pressure (e.g. 7 Torr) while the hot-zone was heated to the required temperature (220 °C). Next, the substrate was cooled and held at a lower temperature T_{sub} (−15 °C). After allowing an hour for the system to approach thermal equilibrium, monomer and initiator were introduced into the chamber at set flowrates. For all experiments, the monomer flow rate was fixed at 4 sccm and monomer/initiator feed molar ratio was adjusted by changing the flow rate of initiator. After the deposition was complete, the chiller and mass-flow controllers were turned off. The reactor chamber was pumped down for an additional half an hour to ensure complete removal of unreacted monomers. Table 1 lists the experimental conditions of 21 different experimental runs, and Fig. 2 indicates the different types of reactor hot-zones used. Each set of experiments was designed to study different process variables: hot-zone configuration, hot-zone temperature, reactor base-pressure, substrate temperature and initiator flowrate.

2.4. Characterization of i-CVD films

Fourier transform infrared spectroscopy (FT-IR, Brüker IFS/66) was used to confirm the structure and composition of polymer films. Spectra were acquired directly from as-deposited PMMA films using KBr substrates at 4 cm^{-1} resolution over the range of 650–4000 cm^{-1} and averaged over 16 scans. For comparison, a PMMA (Sigma Aldrich, $M_n = 69{,}000$ g/mol) standard was dissolved in tetrahydrofuran and solution-cast onto a PTFE IR substrate. Thermal Analysis (PerkinElmer, Pyris) was performed on as-deposited films at a heating rate of 10 °C/min. White light interferometry (Zygo 100) was used to observe the film surface morphology and to measure film thickness and deposition rates. The thickness was averaged from measurements of three different substrate positions. Film thickness results from interferometry were confirmed

Table 1
Deposition conditions and reactor configurations of i-CVD experiments[a]

Experimental run sets	Hot-zone configuration[b]	Hot-zone temperature T_{hot} [°C]	Reactor pressure [Torr]	Substrate temperature T_{sub} [°C]	Flow rate of TBPO initiator [sccm]
Base-case	**A2**	220	7	−15	1
A	**A1**, **A2**, **A3**	220	7	−15	1
B	**A2**	110, 150, 180, 200, 220	7	−15	1
C	**A2**	220	0.1, 0.5, 1, 3, 5, 7, 10, 15	−15	1
D	**A2**	220	7	−15, −10, −5, 0, 5, 10, 15	1
E	**A2**	220	7	−15	1, 2

[a] Flow rate of monomer is kept at 4 sccm, the distance between hot-zone and substrate is 7.62 cm.
[b] See Fig. 2.

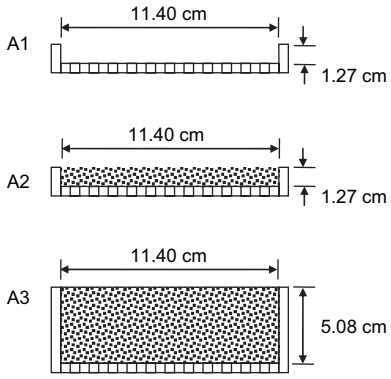

Fig. 2. Hot-zone configurations employed in i-CVD experiments. Hot-zones differ in cylinder height; **A2** and **A3** were packed with glass beads (6 mm diameter) to promote gas mixing and heat transfer.

by an optical film measurement device (Filmmetrics, model: F20). The molecular weight of as-deposited films was determined by using an Agilent 1100 HPLC system equipped with a Viscotek triple detector array. For each sample, the film was dissolved from the substrate using *N*-Methylpyrrolidone (NMP, Sigma Aldrich). Polymer solutions (1 mg/mL) were prepared and filtered prior to injecting 100 μL of the solution into the GPC system, containing three columns (two Viscotek Mixed Bed Low MW i-series and one mixed bed medium MW i-series column) maintained at 60 °C. The software (OmniSEC, Viscotek) calculated the number-average molecular weight M_n, weight-average molecular weight M_w, and the degree of branching of the as-deposited films. Molecular weight was obtained by integration of GPC traces. Branching was calculated using the Zimm–Stockmayer model [30] where the structure factor, relating the hydrodynamic radii to the radii of gyration, was chosen to be 0.75. Results were calibrated using a set of narrow poly(methyl methacrylate) standards of known molecular weight and molecular weight distribution.

3. Results and discussion

Several PMMA films were successfully deposited from methyl methacrylate (MMA) and *t*-butyl peroxide (TBPO) as an initiator using the base-case conditions listed in Table 1. A control experiment (without TBPO initiator) was also carried out and no deposition was observed. Typical thicknesses of as-deposited films were about 3 μm after 8-h depositions. Film thickness measurements on a 3-inch-diameter silicon wafer show good uniformity with deviation only 2% over 28 different positions. Resulting films exhibit relatively smooth, featureless surfaces. The RMS roughness, as determined by interferometry, is around 20 nm (data not shown) which is an order of magnitude larger than the resolution of the instrument. Films are easily dissolved from surfaces using a good solvent for PMMA such as tetrahydrofuran (THF). From thermal analysis, the as-deposited polymer shows a glass transition temperature (T_g) of 105 °C and undergoes thermal decomposition at around 275 °C (data not shown). These thermal characteristics agree well with PMMA standards [31].

Fig. 3 shows FT-IR spectra of PMMA standard (a) and as-deposited film (b). They show the excellent agreement of both peak positions and peak area ratio. The film exhibits characteristic absorption bands expected for PMMA: C–O stretching (1240 cm^{-1}), C–H bending (1452 cm^{-1}), C=O stretching (1730 cm^{-1}) and C–H stretching (2990 cm^{-1}). The spectrum shows no evidence of alkene groups at 1646 cm^{-1} indicating that all condensed monomers either reacted to form PMMA or evaporated and were removed from the film following deposition.

Using base-case operating conditions, the number-average molecular weight of as-deposited polymer was measured to be 25,000 Da. This molecular weight is comparable to the molecular weight of as-deposited polymer using the hot-filament reactor designs [21]. The polydispersity index (PDI) is around 1.4 which is relatively low compared to conventional radical polymerization in solution [32]. The low polydispersity in i-CVD process is attributed to bulk free radical polymerization in the absence of solvent, which limits chain-transfer. In addition, the mobility of polymer chains decreases with increasing molecular weight. As a result, short polymer chains grow faster than long polymer chains, leading to a slightly lower molecular weight distribution. The as-deposited films also show little branching compared to the linear PMMA standard. This indicates that the hot-zone reactor design limits undesirable monomer degradation that could result in branching and shorter chain polymers. The hot-zone reactor design is capable of making high quality polymer films.

The growth of glassy PMMA films reported here can be compared to a recent study by Chan and Gleason resulting in hot-filament i-CVD growth of PMMA. In Chan's study, polymer films could not be grown using *t*-butyl peroxide (TBPO) as the initiator. It is possible that low molar mass polymer was deposited, but no material remained after vacuum drying. However, high molar mass PMMA films were grown ($\sim$20 nm^{-1} min) using triethylamine (TEA) as an

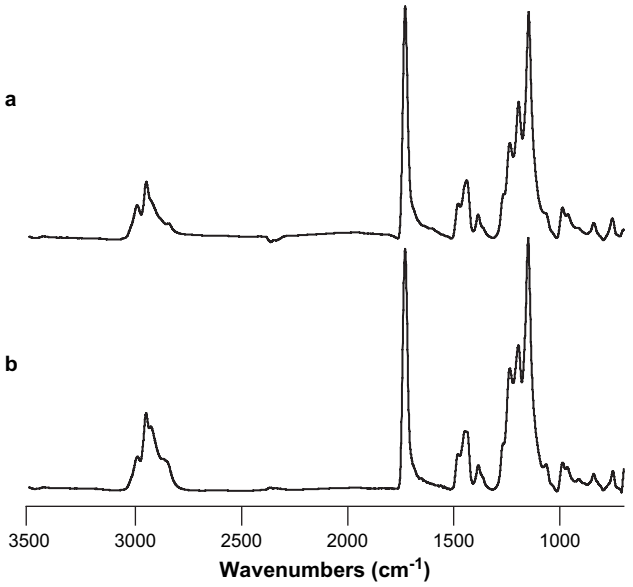

Fig. 3. FT-IR spectra of (a) PMMA standard from Sigma Aldrich and (b) PMMA deposited using axisymmetric i-CVD reactor.

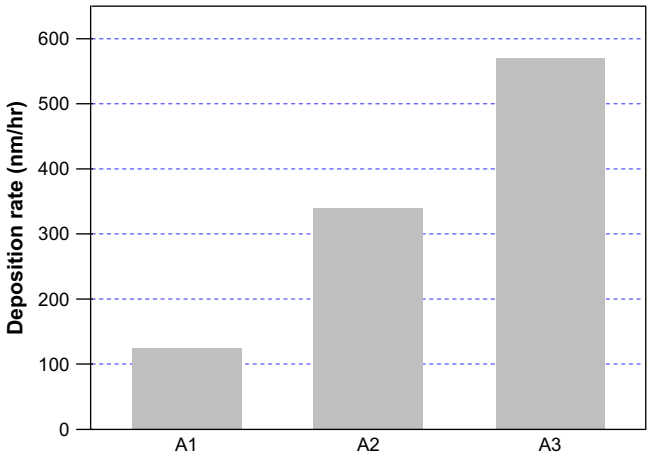

Fig. 4. PMMA deposition rates for different reactor hot-zones in axisymmetric i-CVD reactor operating under base-case conditions (hot-zone temperature: 220 °C).

initiator [15]. TEA requires much higher temperatures for dissociation into free radicals, and, to achieve this, the hot-filament in the i-CVD reactor was heated to 550 °C. The authors deduced that a higher filament temperature is necessary to support the propagation kinetics of the monomer. In the current study, high molecular weight PMMA thin films can be grown using TBPO and a relatively low hot-zone temperature of 220 °C as indicated in Fig. 4. This finding suggests that either the hot-zone is more effective in generating free radicals, or that generated radicals are more efficiently delivered to the target substrate due to the reactor geometry and the low substrate temperature.

Initiated CVD of PMMA using the axisymmetric reactor can be broken into three steps: (1) thermal initiation inside of the hot-zone; (2) monomer and free radical mass transport from the hot-zone to the substrate; and (3) reagent condensation and polymerization that occurs on the substrate. Experiments (sets A–E in Table 1) were designed to study each of these steps. The results led to the development of simple physical models that describe, qualitatively, the physics occurring in each reactor region.

3.1. Hot-zone configuration and temperature

To better understand the efficiency of the hot-zone in activating initiator molecules, three different hot-zone designs were implemented as shown in Fig. 2. Comparing deposition rates from an unpacked (**A1**) to a packed (**A2**) hot-zone shows that packing with glass beads significantly increased the deposition rate, by over a factor of two. Although the residence time is significantly lower for the packed hot-zone **A2** (0.25 s) compared to hollow hot-zone **A1** (0.7 s), the glass spheres greatly increase the thermal contact area, promoting free-radical formation. The highest deposition rate of 570 nm/h was observed for configuration **A3** involving a packed hot-zone with an extended length. In comparing **A2** to **A3**, the reactor length was extended by a factor of four, but the deposition rate increased less than a factor of two. This suggests that configuration **A3** is approaching the equilibrium conversion of initiator to free radicals at the outlet of the hot-zone.

To further study thermal initiation in the i-CVD reactor, PMMA coatings were deposited at different hot-zone temperatures using reactor configuration **A2**. Other process conditions were held constant and are summarized in Table 1. As shown in Fig. 5, the measured film deposition rate increases about an order of magnitude with increasing hot-zone temperature. Data can be fitted using an Arrhenius relationship, and the resulting slope indicates an apparent activation energy of 97 kJ/mol. This value is significantly less than the literature reported *t*-butyl peroxide activation energy of 153 kJ/mol [33]. This difference is attributed to three factors: (1) initiator molecules never achieve thermal equilibrium within the hot-zone; (2) some recombination of free radicals may occur in the volume between the hot-zone and the substrate; and (3) additional recombination of primary radicals may occur on the target substrate.

To summarize, the measured deposition rate is indirectly related to the rate of initiator dissociation. While homolytic cleavage of the TBPO peroxy bonds occurs within the hot-zone, only a fraction of the resulting primary free radicals adsorb on the target substrate and contribute to film growth. It is not surprising that many generated free radicals are lost. Compared to solution polymerization, the initiator-to-monomer molar feed ratio (1:4) is very high, and consequently, some recombination of gas and surface primary free radicals is expected. Inasmuch as primary radicals can undergo recombination, they can also terminate growing polymer chains. These events can influence the polymerization kinetics in i-CVD films [18].

This study introduces the packed hot-zone as an alternative to the resistively-heated hot-filament free radical source traditionally used in i-CVD processing. Thermal control of the hot-zone is simple and precise. Compared to the hot-filament, the packed hot-zone has a far greater thermal mass

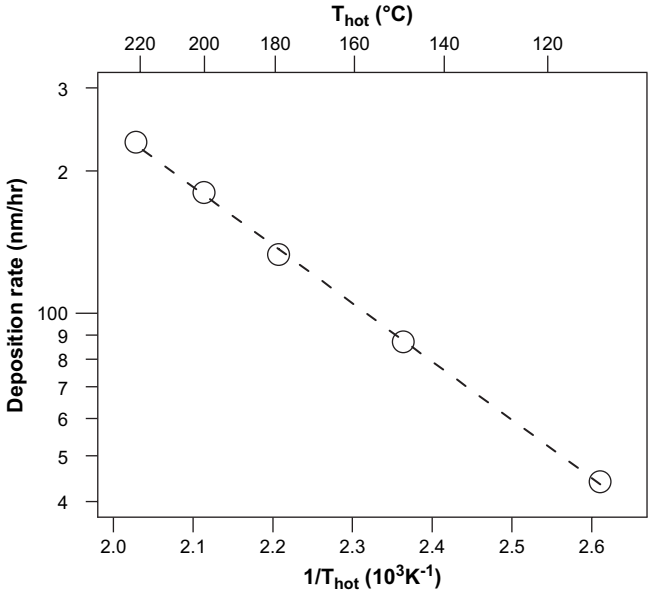

Fig. 5. Logarithmic plot of PMMA deposition rate versus hot-zone temperature. Points indicate measured deposition rates at different hot-zone temperatures, and dashed line shows a least-squares Arrhenius-fit to the data.

and eliminates temperature gradients that are suspected around filament edges. The elimination of hot-spots may be an important factor when considering undesirable high-temperature side-reactions. For the experimental conditions considered here, the kinetics of initiator dissociation within the hot-zone appear to be a key rate-limiting step for PMMA deposition. Interestingly, this observation is in contrast to a recent hot-filament i-CVD study of poly(alkyl acrylates) [17,18] where the deposition rate was found to depend weakly on hot-filament temperature, with activation energy of only ~12 kJ/mol.

3.2. Reactor pressure

Fig. 6a shows the effect of reactor base-pressure on measured deposition rates. The data show a maximum deposition rate (325 nm/h) at pressures about 7 Torr. The maximum can be explained on the basis of the reactor residence time, which is directly proportional to pressure. At low pressures, gases quickly pass through the hot-zone, and the extent of primary radical generation is low. At high pressures, gases pass slowly through the hot-zone, leading to higher levels of initiation. However, due to lower gas velocities, recombination of free radicals becomes significant in the volume between the hot-zone and the substrate.

A crude and simplified plug-flow model illustrates these effects and explains, qualitatively, the rise and fall in deposition rate. This model was used to generate the least-squares fit shown in Fig. 6a. In this model, flow through the i-CVD system is divided into two isothermal tubular reactors: a hot-zone (HZ) and a recombination-zone (RZ) reactor. A gas stream containing initiator molecules (I_2) is fed to the hot-zone where thermal initiation occurs. Recombination is only permitted in the recombination-zone, and the polymer deposition rate is taken as proportional to the number of generated free radicals that pass through the RZ without undergoing recombination.

In the hot-zone, initiator molecules are thermally activated, leading to the formation of primary free radicals:

$$I_2 \rightarrow 2I\bullet, \tag{1}$$

where I_2 refers to initiator molecules, and I• denotes primary free radicals. The reverse reaction occurs in the recombination-zone. Since initiation is a unimolecular process, the reaction is taken as first order

$$r_i = -k_i C_i, \tag{2}$$

where C_i is the gas concentration of I_2 and k_i is the initiation rate constant. The plug-flow design equation relating the hot-zone length L_{HZ} to the degree of initiator conversion X_i is

$$L_{HZ} = -\frac{C_{i0} v_{0,HZ}}{a_x} \int_0^{X_i} \frac{dX_i}{r_i}, \tag{3}$$

where C_{i0} is the initial inlet initiator concentration, $v_{0,HZ}$ is the total volumetric flow rate to the hot-zone, and a_x is the reactor

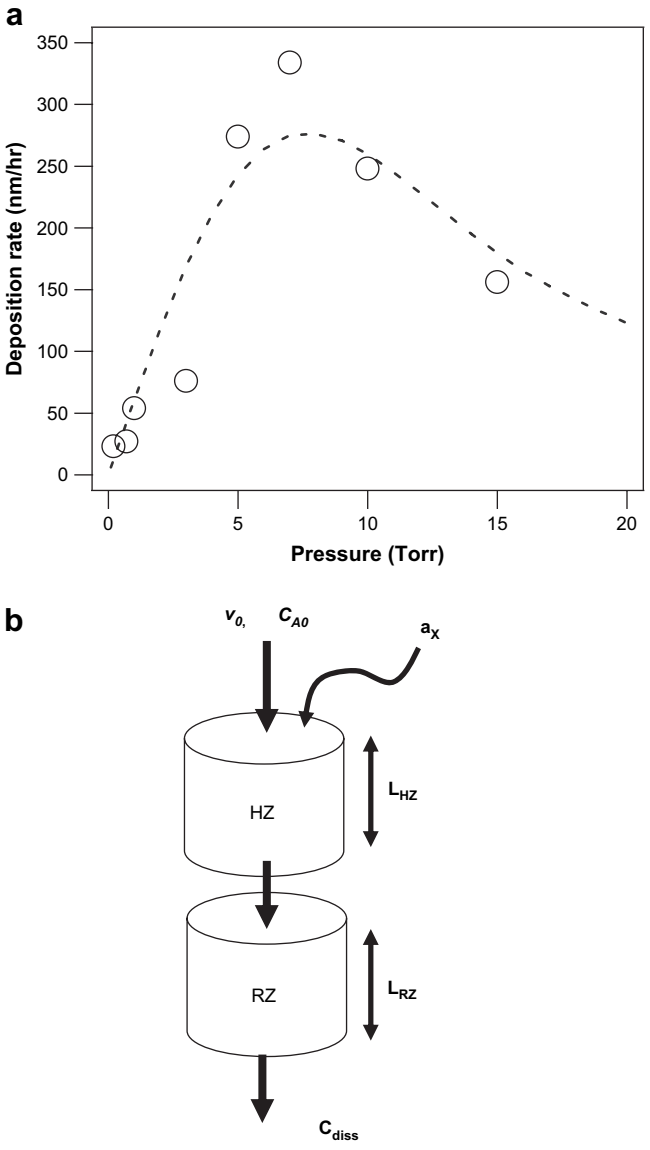

Fig. 6. (a) Experimental results (○) and model fit (dashed line) illustrating the relationship between deposition rate and reactor base-pressure and (b) simplified plug-flow reactor diagram involving one reactor for thermal initiation and a second reactor for recombination. Model constants include $k_i = 1.0 \times 10^{-5}$ s^{-1}, $L_{HZ} = 1.26$ cm, $L_{RZ} = 6.0$ cm, $a_x = 102.6$ cm^2, and $C_{i0} = 5.9 \times 10^{-7}$ mol/cm^3, with least-squares fitted parameters $k_r = 7.0 \times 10^8$ L/mol s, and $\beta = 1.5 \times 10^8$.

cross-sectional area. Since initiation creates additional gas molecules, the concentration of I_2 decreases with conversion as

$$C_i = C_{i0}\left(\frac{1 - X_i}{1 + X_i}\right). \tag{4}$$

Combining Eqs. (2)–(4), and integrating, results in

$$L_{HZ} = v_{0,HZ}/k_i a_x[-X_i - 2\ln(1 - X_i)]. \tag{5}$$

This equation relates the hot-zone reactor length to the chemical conversion. A similar procedure is repeated for the recombination reaction which is described using a second-order rate law:

$$r_{i\bullet} = k_r C_{i\bullet}^2, \tag{6}$$

where k_r is the recombination rate constant, and $C_{i\bullet}$ is the concentration of free radical species. If the inlet concentration of free radicals $C_{i\bullet,in}$ is taken as the product, $C_{i0}X_i$, this results in

$$L_{RZ} = \frac{v_{0,HZ}(1+X_i)}{k_r a_x C_{i0}}\left[-\frac{1}{2}\ln(1-X_r) + 1/4X_r + X_r/4(1-X_r)\right], \tag{7}$$

relating the length of the recombination-zone, L_{RZ}, to the fraction of generated free radicals that undergo recombination, X_r.

Since all experiments were conducted at a fixed molar feed rate, C_{i0} can be calculated using the ideal gas law. Eqs. (5) and (7) then relate operating pressure to the outlet concentration of primary free radicals $C_{i\bullet,out} \sim C_{i0}X_i\ (1-X_r)$. Again, this quantity is assumed to be proportional to the polymer deposition rate.

The dashed line in Fig. 6 represents a least-squares fit to experimental data using the simplified plug-flow model. Parameters include two reaction constants (k_i, k_r), three reactor dimensions (L_{HZ}, L_{RZ}, and a_x) and a proportionality constant, β, that relate the deposition rate to the outlet concentration of primary free radicals. The reactor dimensions are known, and k_i is around 10^{-5} s^{-1} which was estimated from the literature [34], leaving only two unknowns (k_r and β) to be fitted. Note that the fitted value of k_r (7.03×10^8 L/mol s) is in rough agreement with measurements of small radical recombination rates [35]. The quality of fit is reasonable and suggests that, at low pressure, deposition rate is determined by thermal initiation, and, at high pressure, recombination cannot be neglected.

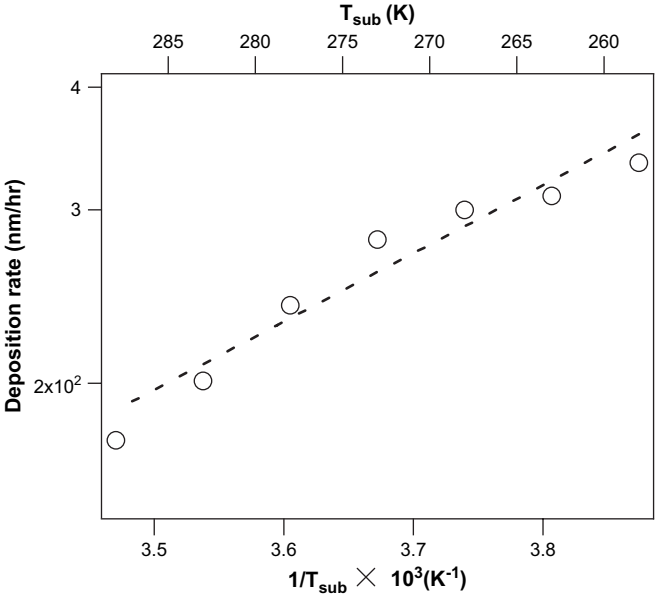

Fig. 7. Plot showing deposition rate dependence on substrate temperature, T_{sub}. Dashed line shows a least-squares Arrhenius-fit to the data with a slope corresponding to a negative activation energy of −12 kJ/mol. The hot-zone temperature was held at 220 °C and reactor base-pressure was 7 Torr.

3.3. Substrate temperature

The measured polymer deposition rate also depends on the substrate temperature T_{sub}. A semi-logarithmic plot of deposition rate versus $1/T_{sub}$ is shown in Fig. 7. The data are nearly linear, and a least-squares fit corresponds to an activation energy of −12 kJ/mol. On the one hand, a negative activation energy is expected because lower substrate temperatures lead to higher levels of monomer adsorption, hence faster polymerization. Such adsorption-limited kinetics were observed in analogous hot-filament reactor studies [18]; though, a much higher activation energy was reported (−79.4 kJ/mol).

In the present study, diffusive transport of primary free radicals is also believed to limit deposition. In all experiments inertial forces are on the same scale as viscous forces. For example, the dimensionless Reynolds number, reflecting the ratio of inertial forces to viscous forces, is about 0.7 for the base-case condition (calculated using the Kinetic Theory of Gases at a temperature of 400 K). This suggests that diffusive

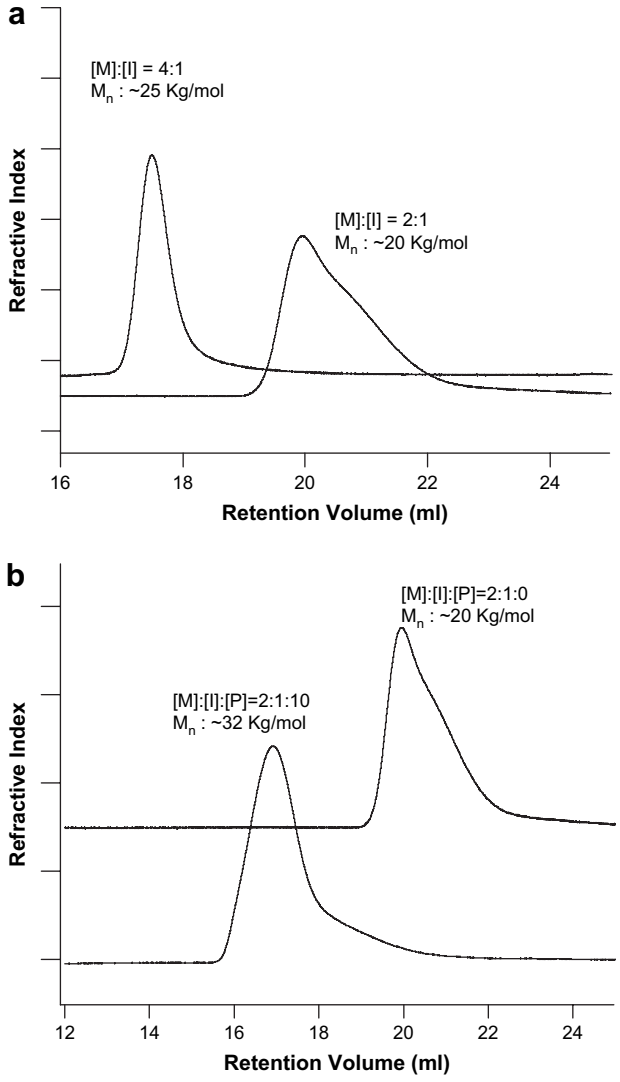

Fig. 8. Size exclusion chromatograms of vapor deposited PMMA: (a) effect of monomer/initiator molar feed ratio and (b) effect of non-reactive third component, 1-butanol.

phenomena play important roles in mass, momentum, and thermal transport and that there are no boundary layers. Furthermore, the Kinetic Theory of Gases provides scaling expressions for diffusion coefficients. In particular, the mass diffusion coefficient scales as $T^{3/2}$. A lower substrate temperature can therefore reduce the gas phase temperature and the diffusive flux of free radicals to the substrate. Opposite to this effect, a lower substrate temperature increases monomer adsorption, promoting polymerization and film deposition [18]. A balance of these two effects determines the observed deposition rate and explains the reduced sensitivity to substrate temperature reported here.

3.4. Monomer/initiator molar feed ratio

Size exclusion chromatography was used to assess the molecular weight of several deposited films. Typically films exhibit molecular weights of about 20 kg/mol. The molecular weight of as-deposited PMMA polymer could be adjusted using two methods. By changing the monomer/initiator feed molar ratio from 2:1 to 4:1, the number-average molecular weight increased from 20 to 25 kg/mol (Fig. 8a). A high concentration of free radicals may terminate growing polymer chains, resulting in the low molecular weight polymer. The effects of introducing a non-reactive, third component into the feed gases is shown in Fig. 8b. By introducing the 1-butanol into the system, the molecular weight of as-deposited film increases from 20 to 32 kg/mol. Since i-CVD reaction involves bulk polymerization, as chains grow longer, they lose mobility. The introduction of 1-butanol is believed to improve the mobility of free radical end-groups, acting as a solvent.

4. Conclusions

This study demonstrates that poly(methyl methacrylate) films can be deposited using an axisymmetric i-CVD technique. Mixtures of monomer, methyl methacrylate and initiator, *t*-butyl peroxide were fed into a vacuum reactor containing a hot-zone and back-cooled substrate. The resulting as-deposited films have smooth surfaces and exhibit molecular weights ranging from 20 to 32 kDa. Several reactor design parameters were studied to understand film growth limitations. An Arrhenius relationship (with slope 97 kJ/mol) between the deposition rate and the hot-zone temperature indicates that polymer growth is limited by thermal initiation of free radicals. High deposition rates require good thermal contact between the hot-zone and feed gases. Upon increasing the reactor pressure, the rate of film growth rate exhibits a maximum that is explained using a simple tubular reactor model. At low pressures, free-radical initiation is inefficient in the hot-zone, and at high pressures, recombination of free radicals above the substrate limits film growth rate. Higher film growth rates were also observed upon decreasing the substrate temperature. These data suggest that deposition is limited by two effects: monomer adsorption on the substrate and free radical diffusion to the substrate. As expected, increasing the monomer-to-initiator molar feed ratio increased molecular weight. Similar effects were observed by introducing a third, non-reactive, component (1-butanol).

References

[1] Martin TP, Kooi SE, Chang SH, Sedransk KL, Gleason KK. Biomaterials 2007;28(6):909–15.
[2] Pyo SW, Lee DH, Koo JR, Kim JH, Shim JH, Kim JS, et al. Synthetic Metals 2005;154(1–3):141–4.
[3] Zaharias GA, Shi HH, Bent SF. Thin Solid Films 2006;501(1–2):341–5.
[4] Dimov D, Strijkova V, Karamancheva I, Zhivkov I, Tsenov I, Spassova E, et al. Journal of Optoelectronics and Advanced Materials 2005;7(3):1445–9.
[5] Roualdes S, Sanchez J, Durand J. Journal of Membrane Science 2002;198(2):299–310.
[6] Sato M, Iijima M, Takahashi Y. Thin Solid Films 1997;308:90–3.
[7] Anthamatten M, Letts SA, Day K, Cook RC, Gies AP, Hamilton TP, et al. Journal of Polymer Science Part A: Polymer Chemistry 2004;42(23):5999–6010.
[8] Salem JR, Sequeda FO, Duran J, Lee WY, Yang RM. Journal of Vacuum Science & Technology A: Vacuum Surfaces and Films 1986;4(3):369–74.
[9] Takahashi Y, Iijima M, Inagawa K, Itoh A. Journal of Vacuum Science & Technology A: Vacuum Surfaces and Films 1987;5(4):2253–6.
[10] Chen XC, Anthamatten M, Harding DR. Macromolecules 2006;39(22):7561–5.
[11] Tsai FY, Blanton TN, Harding DR, Chen SH. Journal of Applied Physics 2003;93(7):3760–4.
[12] Ojeda JR, Martin DC. Macromolecules 1993;26(24):6557–65.
[13] Gies AP, Nonidez WK, Anthamatten M, Cook RC. Macromolecules 2004;37(16):5923–9.
[14] Chan K, Gleason KK. Langmuir 2005;21(19):8930–9.
[15] Chan K, Gleason KK. Chemical Vapor Deposition 2005;11(10):437–43.
[16] Chan K, Gleason KK. Macromolecules 2006;39(11):3890–4.
[17] Lau KKS, Gleason KK. Macromolecules 2006;39(10):3695–703.
[18] Lau KKS, Gleason KK. Macromolecules 2006;39(10):3688–94.
[19] Lau KKS, Murthy SK, Lewis HGP, Caulfield JA, Gleason KK. Journal of Fluorine Chemistry 2003;122(1):93–6.
[20] Loo LS, Gleason KK. Electrochemical and Solid-State Letters 2001;4:G81–4.
[21] Mao Y, Gleason KK. Langmuir 2004;20(6):2484–8.
[22] Mao Y, Gleason KK. Langmuir 2006;22(4):1795–9.
[23] Gross S, Camozzo D, Di Noto V, Armelao L, Tondello E. European Polymer Journal 2007;43(3):673–96.
[24] Tsai F-J, Torkelson JM. Macromolecules 1990;23:4983–9.
[25] Tsai F-J, Torkelson JM. Macromolecules 1990;23:775–84.
[26] Avramescu ME, Sager WFC, Mulder MHV, Wessling M. Journal of Membrane Science 2002;210:155–73.
[27] Caquineau H, Menut P, Deratani A, Dupuy C. Polymer Engineering & Science 2003;43:798–808.
[28] Nakanishi H, Satoh M, Norisuye T, Tran-Cong-Miyata Q. Macromolecules 2006;39(26):9456–66.
[29] Jansen BJP, Rastogi S, Meijer HE, Lemstra PJ. Macromolecules 2001;34:3998–4006.
[30] Zimm BH, Stockmayer WH. Journal of Chemical Physics 1949;17(12):1301–14.
[31] Wunderlich W. In: Brandrup J, Immergut EH, Grulke EA, editors. Polymer handbook, vol. V. New York: John Wiley & Sons; 1999. p. 87.
[32] Odian G. Principles of polymerization. Hoboken: John Wiley & Sons; 2004.
[33] Perona MJ, Golden DM. International Journal of Chemical Kinetics 1973;5:55–65.
[34] Batt L, Benson SW. Journal of Chemical Physics 1962;36(4):895–901.
[35] Hiatt R, Benson SW. Journal of the American Chemical Society 1972;94:6886–8.